

The Origin of Micro-Loading Effect of TEOS-O3 Oxide II

U-In Chung, Myoung-Beom Lee, In-Seon Park, Sang-In Lee and Moon-Yong Lee

Semiconductor R&D Center, Samsung Electronics Co., San#24 Nongseo-Lee,
Kiheung-Eup, Yongin-Gun, Kyunggi-Do, KOREA

TEOS-O3 oxide shows a strong deposition rate dependence on the underlying materials and underlying pattern structure. In this work, the pattern dependence(' micro-loading effect ') is examined by observing the TEOS-O3 oxide profile in 100umX100um metal pad. Micro-loading effect of TEOS-O3 oxide becomes more severe as the deposition power of underlying plasma oxide increases. Also, the deposition rate of TEOS-O3 oxide increases with the B or BF2 implantation does. It decreases with P or As implantation does. The deposition rate increases with increasing implantation energy in case of P or As and with decreasing of implantation energy in case of B or BF2. From the results, it is proposed that the origin of micro-loading effect is attributed to an electronegative nature of the intermediates during TEOS-O3 oxide deposition.

1. INTRODUCTION

In sub-half micron technology, the dielectric planarization process in multilevel metallization technology becomes more important because a nearly perfect planarization is needed to overcome the following lithography process. Also, as the metal pitch decreases less than 1um, the filling between the metal lines becomes more difficult. Among many kinds of oxide for gap filling and planarization, TEOS-O3 oxide is one of the candidates for those purpose.

However, TEOS-O3 oxide shows a strong deposition rate dependence on the underlying materials and underlying pattern structure(1) as well as the tendency of water absorption. Many researchers have published to remove the underlying material dependence, for example, by two step deposition(2), ethanol treatment(3), NH3 plasma treatment (4) and HCl/H2O2 treatment(5).

In this study, the pattern structure dependence('micro-loading effect') that the deposition profile on the pattern is different depending on the pattern geometry is examined by observing the TEOS-O3 oxide profile in 100umX100um metal pad. And, the deposition mechanism of TEOS-O3 oxide is proposed.

2. EXPERIMENTAL

Figure 1(a) and 1(b) show experimental procedure of this work. The metal structure is Ti(300Å)/TiN(600Å)/AlSiCu(6000Å)/TiN(250Å). Metal film was dry etched by conventional MERIE method. To investigate the effect of underlying plasma oxide on the micro-loading effect, prior to the deposition of TEOS-O3 oxide, the deposition power and precursor (SiH4 and TEOS) of plasma capping oxide were changed. TEOS-O3 oxide was prepared in APCVD apparatus. The concentration of ozone was 5% and TEOS(N2 carrier)/O2 flow ratio was 0.3. The deposition temperature was 400C. After deposition of TEOS-O3 oxide, the deposition profile was observed at various metal pads, such as isolated pad ('typeA pad'), continuity pad('type B pad') which is floated electrically and continuity pad connected to N+ and P+ diffusion layer('type C pad') as shown in Fig.1(a).

In order to confirm the origin of micro-loading effect, the deposition rate dependencies with ion implantation species(P, B, BF2 and As), energies(30KeV - 150KeV) and doses(3E13/cm2 - 3E15/cm2) was studied as shown in Fig.1(b). 100Å thermally grown oxide was used as implantation screen oxide. Also, to examine the effects of activation of implanted species and screen thermal oxide on the deposition rate of TEOS-O3 oxide was measured with and without the activation and the screen oxide.

3. RESULTS and DISCUSSION

Fig.2 shows the deposition profile of TEOS-O3 oxide with RF power in the case of Pe-SiH4 oxide capping layer. The micro-loading effect(the thickness of TEOS-O3 oxide at metal pad corner is higher than that at other pad position) in type B pad becomes more severe with RF power. The

micro-loading effect is not found in type A pad. Fig.3 is optical micrographs corresponding to Fig.2. The distinctive difference between type A pad and type B pad can be noticed by pad color difference. The phenomenon that the micro-loading effect depends on the RF power and the kinds of pad is also found in the case of Pe-TEOS oxide as a capping layer as shown in Fig.4. It was also noted that this micro-loading effect is getting severer with decrease of metal line space in type B pad. Fig.5 shows an optical micrographs after TEOS-O₃ oxide deposition at Pe-TEOS oxide as a capping layer at type B pad and type C pad (metal contact to N⁺ diffusion can not be seen due to magnification). Depending on whether the metal pad is connected to N⁺ diffusion or not, the color on pad is remarkably different even at the identical pattern geometry, which means that the micro-loading effect is closely related to the charging on pad. The charge on pad is generally known to be concentrated to the pad corner and its polarity is positive. The charge can be generated during metal etching and/or Pe-oxide deposition. Thus, it is believed that intermediates of TEOS-O₃ oxide during deposition has a negative polarity. To verify that intermediates have its nature as a negative charge, the deposition rate of TEOS-O₃ oxide was investigated with ion implantation species and implanting conditions.

Fig.6 is deposition rate with the implanted ions, does and energy after removal of thermally grown oxide in Fig.1(b). In the case of phosphorus, the deposition rate increases with does at 30KeV. And it decreases with energy at 3E15/cm² ion does. In the case of boron, the trend is reverse compared to phosphorus. Particularly, the effect of implantation is not found when activation treatment is not done irrespective of ion species. In the case of As and BF₂, the trend is very identical to phosphorus and boron, respectively. Therefore, Fig.6 indicates that the deposition rate depends on the type of majority carrier(electrons in P and As and hole in B and BF₂) and the amount of carrier at Si surfaces, which can be attributed to the electronegative nature of intermediates. Fig.7 is the deposition rate on the thermally grown oxide. As shown in Fig.7, the deposition rate increases with the damage in oxide (the amount of damage increases with does and energy) regardless of ions. Because the positive charge in oxide is generated due to ionization of oxide(a large portion of the impact induced electrons escapes from the oxide as shown in Fig.8), the deposition rate increases.

Fig.8 is our model for micro-loading effect of TEOS-O₃ oxide. The positive charge which is generated during the dry etching and deposition of plasma oxide is considered to be accumulated on the metal pad corner. Therefore, the negatively charged TEOS intermediates can be easily deposited on the metal pad corner. It was noted that the intermediates can move on the oxide surface in a range of 10um. Generally the accumulated charge can be removed when metal line is connected to ground level(N⁺ and P⁺). Thus, micro-loading effect is not found in type C pad.

In Fig.8(b), when thermal oxide exists during the deposition of TEOS-O₃ oxide, a large part of the secondary electrons generated during the implantation can not escape from the thermal oxide. The trapped electrons act as a barrier for the deposition of TEOS-O₃ oxide because its negative nature. Thus, the deposition rate decreases with the implantation energy regardless of the implantation because the amount of trapped secondary electron increases with the implantation energy. When the screen thermal oxide is removed, the deposition rate depends on the implantation energy, does and the implanted species. In Fig.(6), the deposition rate increases with the energy in case of P and reverse trend in case of B. This means that the surface concentration of P and B is important when activation heat treatment is performed.

4. CONCLUSION

The origin of micro-loading effect is attributed to the combination of an electronegative nature of the intermediates during TEOS-O₃ deposition and the build-up of positive charge in metal pad corner.

5. REFERENCES

- 1) M.B.Lee et al, The Japan Society of Applied Physics, Extended Abstracts(the 54th Autumn Meeting, 1993) p. 689
- 2) K.Fujino et al, J. Electrochem. Soc., 138(2), p.550 , 1991
- 3) N. Sato et al, J. Appl. Phys., 32, p.110, 1993
- 4) C.K. Kim et al, VLSI Multilevel Interconnection Conf., 1995, in press
- 5) T. Yoshie et al, Extended Abstract of the 1994 International Conference on Solid State Devices and Materials, Yokohama, p. 715. 1994

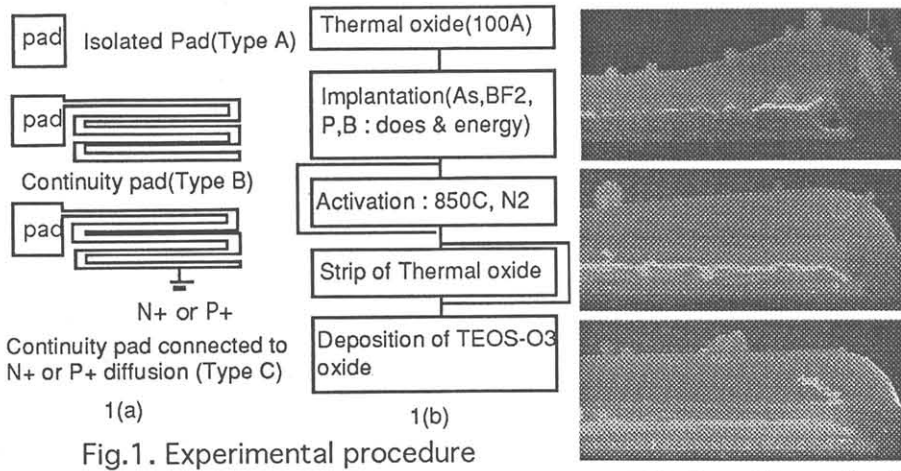


Fig.1. Experimental procedure

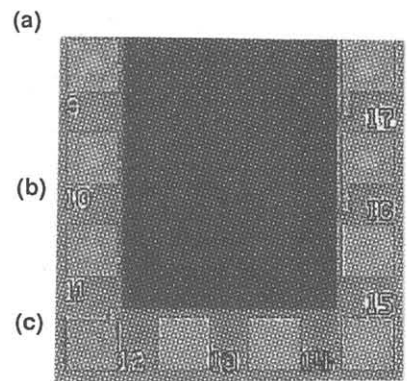


Fig.3. Optical micrograph showing color difference between 'type A' and 'type B' pad. (in case of 150w) ('type A' : 13,14,15,16 pads 'type B' : 9,10,11,12,17 pads)

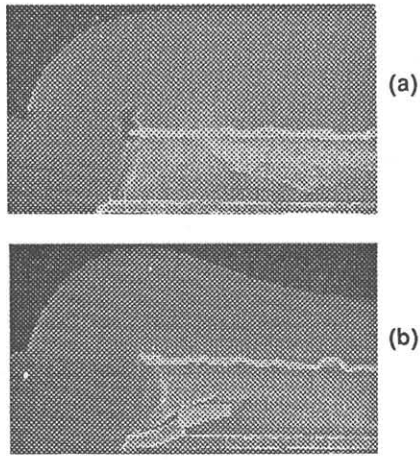


Fig.4. TEOS/O3 oxide profile with RF power of underlying Pe-TEOS ox. ((a): 125watt, (b): 425watt)

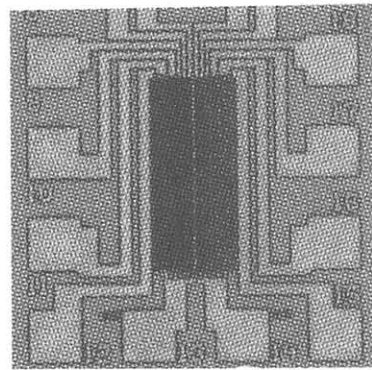


Fig.5. Optical micrograph showing color difference between 'type B' and 'type C' pad. (in case of 425w) ('type B' : 9,10,11,12,13 pads 'type C' : 14,15,16,17,18 pads)

Fig.2. TEOS/O3 oxide profile with RF power of underlying Pe-SiH4 ox. ((a): 300watt, (b):150watt, (c): 100watt)

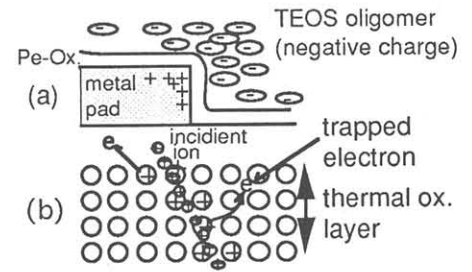


Fig.8. Model for deposition profile at metal pad (a) and deposition rate on the thermal ox. (b) (When thermal oxide exists, deposition rate increases regardless of IIP species due to the trapped electrons in thermal ox. layer. Deposition rate is only dependent on the dose and energy)

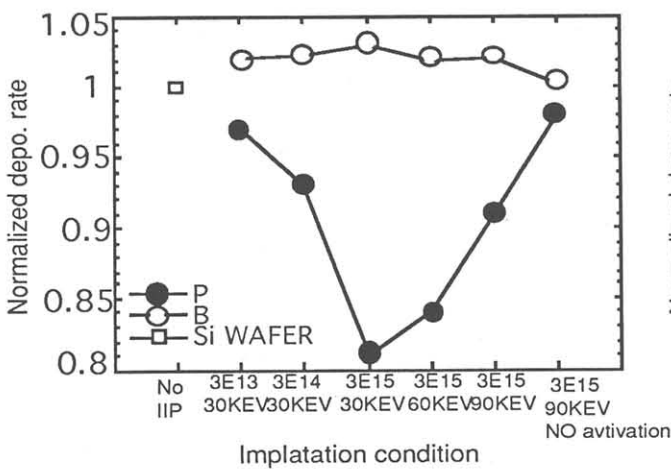


Fig.6. Change of deposition rate after removal of thermal oxide with implantation condition. (activation treatment : 850C, N2, 30min)

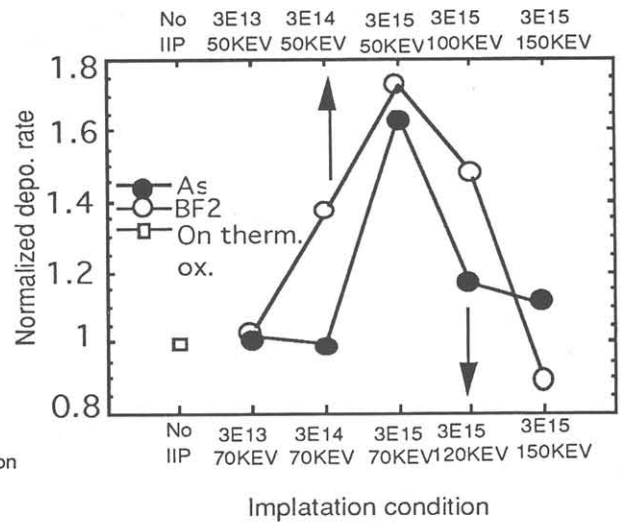


Fig.7 Change of deposition rate on thermal oxide after implantation (activation treatment : 850C, N2, 30min)

